Seismic performance of tunnel lining of side-by-side and vertically stacked twin-tunnels

ARTICLE *in* JOURNAL OF CENTRAL SOUTH UNIVERSITY OF TECHNOLOGY · AUGUST 2011

Impact Factor: 0.36 · DOI: 10.1007/s11771-011-0826-z

2 AUTHORS:

Shong loong Chen
National Taipei University of Technology
29 PUBLICATIONS **38** CITATIONS
SEE PROFILE

Meen-Wah Gui
National Taipei University of Technology (T…
24 PUBLICATIONS **86** CITATIONS
SEE PROFILE

J. Cent. South Univ. Technol. (2011) 18: 1226−1234
DOI: 10.1007/s11771−011−0826−z

Springer

Seismic performance of tunnel lining of side-by-side and vertically stacked twin-tunnels

CHEN Shong-loong(陳水龍)[1, 2], GUI Meen-wah(魏敏樺)[1]

1. Department of Civil Engineering, National Taipei University of Technology, Taipei 10608, Taiwan, China;
2. Department of Civil and Engineering Management, National Quemoy University, Kinmen, Taiwan, China

Abstract: The dynamic interaction between tunnel lining and its surrounding soil is a complicated issue as the magnitude of seismic wave from bedrock to the structure can be easily influenced by the geometrical layout and structural stiffness of the tunnel. A series of numerical analysis was conducted to study the dynamic response of the tunnel lining of side-by-side and vertically stacked double-tube tunnel since the inertia and kinematic interactions between the tunnel lining and the surrounding soil during an earthquake could induce excessive stresses to the lining itself due to the stiffness variation between the lining and the soil. Real earthquake ground acceleration was used as an input motion in the dynamic analysis. The interactive behavior of bending moment and axial forces, and the displacement of the tunnels were used to evaluate the effect of tunnel geometrical layout on the performance of the lining. It is found that the effect of earthquake on the axial thrust of the lining is insignificant, and there is a reduction of the bending moment in the lining due to the redistribution of the surrounding soil after the earthquake.

Key words: underground excavation; tunnel lining design; seismic response; numerical analysis

1 Introduction

Many new infrastructures such as water sewerage system, walkways, and lifelines are now constructed underground. In Taipei, by the end of 2009, about half of the completed 93 km-long Taipei Mass Rail Transit Network (TRTN) was constructed underground; and in Shanghai, by 2010 Shanghai EXPO, some 400 km-long of metro lines will be in operation in which 9 out of 11 lines run through urban central areas [1].

These underground tunnels have been constructed by either the cut-and-cover method or shield tunneling method depending on the geological conditions. The shield tunneling construction is good at eliminating the impact on ground traffic and the environment. A flexible ring, normally formed by six pieces of segmental lining, is fitted around the tunnel circumference created by the shield machine to provide resistance to earth and water pressure. The gap between the excavated surface and the lining is filled with grout to stabilize the excavated surface and to reduce decompaction and bulking that may cause additional surface settlement because of uneven load distribution [2]. This method and segmental lining have been widely used in soft ground in recent years to improve the speed of construction and thus reduce the cost of tunneling; but the lining design is still mainly based on empirical and analytical methods [3−4]. Attention must be given to the economic design of the linings [5] because over-design of pre-cast tunnel lining and the excessive use of steel bar not only increase the cost of the project but also induce complication during the concreting of the lining. The stresses of the reinforcement in the lining of shield tunnel in construction stage were evaluated with the program ADINA [6]. However, the analysis was only based on static loading conditions. It is difficult to assess the validity of current lining design method of Taipei Mass Rail Transit System because there are insufficient instrumentation records on the lining stress−strain performance for comparison purpose. The volume ratio of reinforcement to concrete has been taken to be 0.019−0.052, depending on the tunnel dimension, depth and soil characteristics [7].

Since Taiwan is located in the west Pacific earthquake belt zone, a thorough seismic response analysis based on the historical ground acceleration records must be conducted prior to any detailed design of structures. As the stiffness of the lining and the soil varied significantly during an earthquake event, inertia interaction and kinematic interaction between the lining and the soil could induce excessive stress to the lining itself. The dynamic interaction between the lining and the soil is a complicated issue as the magnitude of seismic

Received date: 2010−03−22; **Accepted date**: 2011−02−15
Corresponding author: GUI Meen-wah, Associate Professor, PhD; Tel: +886−955154891; E-mail: mwgui@ntut.edu.tw

wave from bedrock to the structure can be easily influenced by the structural stiffness, dynamic soil properties, earthquake force, and the geometrical layout of the tunnel. This work aims at studying the dynamic response, in terms of axial thrust and bending moment, of lining in side-by-side and vertically staked twin-tunnel under an input earthquake wave. The result can then be used to verify the dynamic design methodology of tunnel lining.

2 Backgrounds

2.1 Taipei Rail Transit System (TRTS)

TRTS consists of four main lines: 1) Danshui Line, 2) Muzha−Neihu Line, 3) Bannan Line, and 4) Nanshijiao Line. Due to the increase in passenger volume, four new lines: 1) Luzhou Line, 2) Xinyi Line, 3) Songshan Line, and 4) Xinzhuang Line have been planned and designed, and constructions are currently undertaking. The study site is located at a particular section of Xinzhuang Line.

2.2 Ground conditions

Taipei city is located in Taipei basin that was formed by a series of sedimentation events. The formation of the Taipei basin consists of 1−6 m thick top soil or fill material, followed by a 40−60 m thick alluvial deposit, which lies above the Jingmei formation; the Shongsan formation comprises six alternating silty sand and silty clay layers with varying thicknesses, while the Jingmei formation is mainly composed of dense sands and gravels with diameter of up to 30 cm [8].

In total, eight boreholes were drilled at various locations at the study site. The ground water table was found to vary between 1.7 and 3.5 m below the ground level. The average properties of the sub-soils obtained are given in Table 1. Dynamic soil properties such as the shear modulus were obtained from the field via the shooting-down hole technique, in which the direct travel time of body waves (P- and S-waves) along the boundary of a 50 m deep hole was measured. Using the values of P-wave velocity v_p and S-wave velocity v_s obtained from the soil layers, the following dynamic properties can be derived [9]:

$$\begin{cases} G_{dyn} = \rho v_s^2 \\ E_{dyn} = 2G_{dyn}(1+\mu_{dyn}) \\ K_{dyn} = \dfrac{E_{dyn}}{3(1-2\mu_{dyn})} \end{cases} \tag{1}$$

where ρ is the density of the soil; G_{dyn}, E_{dyn} and K_{dyn} are the dynamic shear modulus, dynamic elastic modulus and dynamic bulk modulus, respectively; μ_{dyn} is the dynamic Poisson ratio, which can be obtained from

$$\mu_{dyn} = \frac{1}{2}\frac{(v_p/v_s)^2 - 2}{(v_p/v_s)^2 - 1} \tag{2}$$

The dynamic properties derived from the down-hole tests are listed in Table 1.

2.3 Lining design

For lining design, the loads acting on the lining must include earth and water pressures, dead load, reaction, surcharge and thrust force of shield jacks, backfill grouting pressure, etc [10]. In addition, seismic load should also be considered if the tunnel is used in seismic active areas. The lining design forces such as bending moment, axial thrust and shear force are then determined by using one of the computational methods proposed in Ref.[10]. It is recognized that the three-dimensional condition in the field may be simulated as two-dimensional conditions by either using formulas with superposition of selected design loads or using numerical program with constitutive laws to achieve stresses and strains under elastoplastic conditions [10]. For the evaluation of the effect of earthquake on tunnels, the seismic deformation method, the seismic coefficient method, and the dynamic analysis are commonly used.

After obtaining the lining forces, the amount of reinforcement required in the lining is determined using the limit state design method, in which the design bending moment and axial thrust are factored by the

Table 1 Down-hole test results obtained from study site

Depth/m	Longitudinal wave velocity, v_p/(m·s^{-1})	Transverse wave velocity, v_s/(m·s^{-1})	Dynamic shear modulus, G_{dyn}/kPa	Dynamic elastic modulus, E_{dyn}/kPa	Dynamic bulk modulus, K_{dyn}/kPa	Poisson ratio
0−6.5	444	114	25 100	73 800	348 600	0.464
6.5−10.5	1 430	120	27 900	83 500	3 927 300	0.496
10.5−26.0	1 660	185	69 800	208 300	4 080 100	0.491
26.0−32.5	1 660	250	133 900	398 600	5 726 200	0.488
32.5−35.0	1 660	313	209 900	622 000	5 624 900	0.481
35.0−45.0	1 660	375	301 300	887 800	5 503 000	0.473

respective safety factors. Structural engineers usually described the relationship between the design axial thrust capacity N_u and the design flexural capacity M_{ult} of the lining cross-section using the so-called N_u−M_{ult} curve. The safety for the combined axial thrust and flexural moment is ensured if this combination of forces is located inside the N_u−M_{ult} curve.

2.4 Seismic design criteria

The seismic design criteria adopted are: during a large earthquake the structural lining that experiences inelastic cyclic deformation should be sufficiently ductile to absorb the imposed deformation without losing their capacity to carry static loads, and during a small earthquake the structural lining should stay within the elastic deformation capacity of the structure so that trains can operate normally [2]. Analysis is normally based on a 475-year return period of regression, which has a peak horizontal ground acceleration of 0.18g at the surface [7].

3 Numerical modeling

Numerical analysis has been adopted for analyzing wave propagation in continuous nonlinear media with large deformations because the complicated boundary conditions and soil models involved could not be reasonably accounted for via simple equations [11]. The finite difference program used in this study is FLAC^{2D} that is well suited for modeling such problem [12]. The program adapts the dynamic equations of motion to ensure a stable numerical scheme when the physical system being modeled is unstable [12]. Note that since the tunnels considered here are long tunnels it is reasonable to assume a plane strain or two-dimensional model for the following analysis [13].

3.1 Constitutive models and material parameters

1) Soil

The Mohr-Coulomb elastoplastic model with a non-associated flow rule was chosen to represent the behavior of the soil in this study. Its failure envelope corresponds to a Mohr-Coulomb criterion (shear yield function) with tension cutoff (tension yield function).

In FLAC, the parameters associated with the Mohr-Coulomb model for an undrained analysis are: unit weight γ, undrained shear strength c_u, elastic modulus E, and Poisson ratio. These parameters have been obtained from a series of laboratory tests and are tabulated in Table 2. For dynamic analysis, which involved loading and unloading behavior of soil, the strain dependent shear modulus proposed in Ref.[14] was used in the analysis.

The model is normally used in the method of linear-equivalent frequency domain analysis and therefore is unable to take the nonlinear increment of shear modulus into account in time domain analysis. To reflect this and the hysteretic behavior of soil in a dynamic analysis, MASING's rule [15] together with the extended MASING's criteria [15−17] have been implemented in the analysis.

Theoretically, the soil damping properties can be omitted because in a non-linear soil model analysis, soil damping is directly captured through the hysteretic loading−reloading cycles in the soil model itself [18]. However, FLAC version 5 does not have the capability to capture the strain dependent damping [12]. Since the hyperbolic model is nearly constant at small strains (less than 10^{-6}−10^{-4}), a constant damping ratio has been used instead. Rayleigh damping, which was originally used in the analysis of structures and elastic continua to damp the natural oscillation modes of the system [12], was used in this analysis. The equation, expressed in matrix form, is shown in the following equation [12]:

$$\boldsymbol{C} = \alpha\boldsymbol{M} + \beta\boldsymbol{K} \tag{3}$$

where $\boldsymbol{C}$ is a damping matrix with components proportional to the mass $\boldsymbol{M}$ and stiffness $\boldsymbol{K}$ matrices; α and β are the mass-proportional damping constant and the stiffness-proportional damping constant, respectively. The values of α and β used in this analysis are 0.1 and 2.5, respectively.

As mentioned earlier, the highest groundwater table observed from the site investigation was 7 m below

Table 2 Average soil properties obtained from study site

Thickness/ m	Soil type	Unit weight/ (kN·m^{-3})	Apparent cohesion/kPa	Angle of friction/(°)	SPT 'N' value	Elastic modulus/kPa	Poisson ratio
0−6.5	CL/SM	17.5	23	17	3	2 300	0.4
6.5−10.5	SM	19.7	0	32	5	20 000	0.33
10.5−26.0	CL	19.3	34	14	9	23 000	0.38
26.0−32.5	SM	20.0	0	32	20	33 000	0.3
32.5−35.0	CL	19.8	77	19	14	43 000	0.35
35.0−45.0	SM/ML	20.6	0	32	30	46 000	0.3

CL—Low plasticity silty-clay; SM—Silty sand; ML—Silty sand

ground level. In the analysis, it was, however, modeled by assigning a water table at 1.0 m below the ground level to cater for condition during the raining season.

2) Tunnel lining

The one-dimensional structural beam element in FLAC that is capable in sustaining uniaxial tension and bending [12] has been used to model the behavior of the structural lining. The stiffness of the segmental lining is taken to be E_cI_e [19], where E_c is the elastic modulus of reinforced concrete and I_e is the effective value of the second moment of area of a jointed lining:

$$I_e = I_j + \left(\frac{4}{n}\right)^2 I = 9.53\times10^{-4}\ \text{m}^4/\text{m} \quad (4)$$

where I is the second moment of area of lining per unit length of tunnel; I_j is the effective value of I at a joint in a lining; n is the number of segments in a lining ring. The general properties of this beam element are listed in Table 3.

Table 3 Properties of tunnel lining

Property	Value
Inner radius, R_i/m	5.6
Outer radius, R_o/m	6.1
Thickness/m	0.25
Width/m	1.00
Number of segment joints	6
Concrete strength/(N·mm^{-2})	50
Elastic modulus of concrete/kPa	3.6×10^7
Poisson ratio of concrete	0.17
Unit weight of concrete/(kN·m^{-3})	26.0

3.2 Modeling sequences

Most of the Taipei twin-tunnels are either parallel (side-by-side) or vertically stacked. The effects of the layout of tunnels on the dynamic response of lining are studied. Figures 1(a) and (b) show the 160 m-wide rectangular finite difference meshes created for the analysis. Both the left and right boundaries are fixed in the horizontal direction to represent the free field condition while the bottom boundary is restrained from both the horizontal and vertical movements in both the static and dynamic runs.

A parametric study is carried out to examine the effect of 1) overburden depth (12, 18, and 24 m) for the parallel tunnels, and 2) clear vertical distances (3, 4, 5, and 6 m) between the two vertically staked tunnels where the upper tunnel always has an overburden depth of 12 m, on the dynamic performance of the lining in terms of bending moment and axial thrust. The studied tunnels have an outer diameter of 6.1 m and the pre-cast reinforced concrete lining has a thickness of 25 cm (Table 3).

After achieving the initial stress state of the ground, the mesh elements at the tunnels location are switched to null model to model tunnels excavation and the beam elements inserted at the tunnels circumference to model the lining installation process.

The effects of excavation sequences, the surface settlement trough, peak settlement and associated volume loss are not the objectives of this study and therefore they are not discussed here. The ground acceleration is modeled using the strongest earthquake data recorded between 2001 and 2006 in Taipei. The design earthquake motion is applied to the bottom of the mesh in Fig.1 and it has been de-convoluted so that it represents the acceleration at 45 m below the ground surface [20]. As a result, the input peak acceleration is only about 0.1g (Fig.2) but during shaking it would produce an acceleration of 0.18g at the ground surface. The calculation is often conducted using the program SHAKE [21].

4 Results and discussion

For better understanding of the problem, the

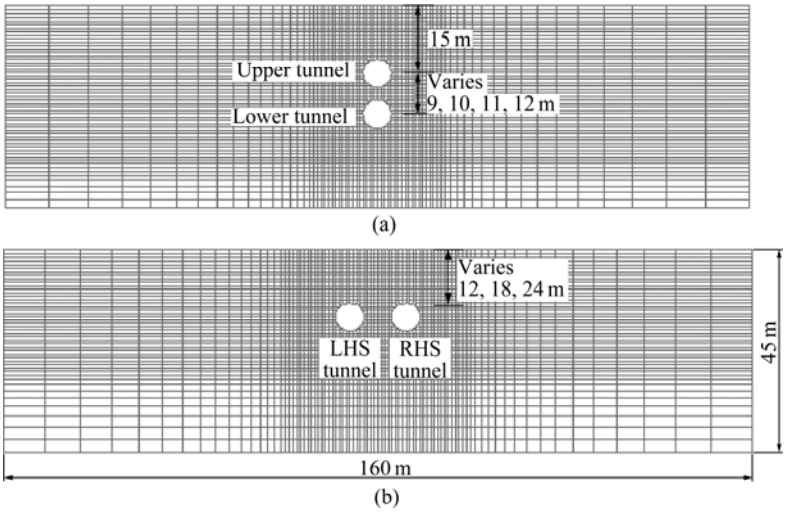

Fig.1 Meshes for study layouts: (a) Vertically stacked; (b) Horizontally placed along side each other

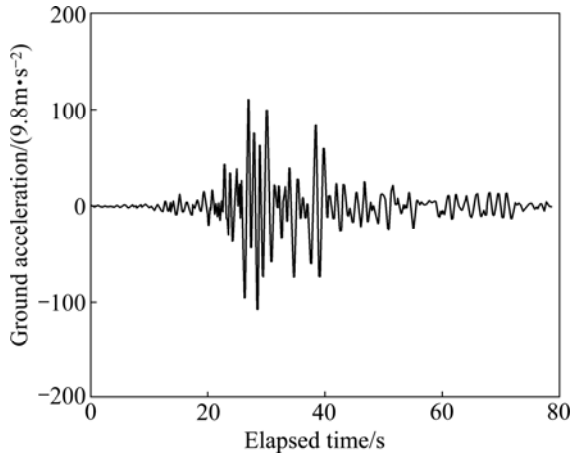

Fig.2 Ground acceleration record used in analysis

influence of tunneling layout and tunneling depth have been performed to understand and, hence, verify the current design approach. The numerical results obtained are presented in time history plots of the maximum lining thrust (inclusive of initial and dynamic stages) and its corresponding bending moment. The recording points are tunnel invert and crown, and the left and right edges of the tunnel.

4.1 Effect of side-by-side layout

Figure 3 shows the time history of axial thrust registered at the invert, crown, and left and right edges of the tunnels. In general, for each of the tunnel depth (12, 18 and 24 m), the axial thrust of the two tunnels are about the same because the tunnels are placed at the same elevation. The axial thrust increases linearly as the tunnel depth increases. For each elevation, the left and right edges of the tunnel sustain the same value of axial thrust; while the invert and the crown sustain different values of axial thrust, especially at the shallower depths. This could be due to the contribution of the lining self-weight but the effect is suppressed as the overburden

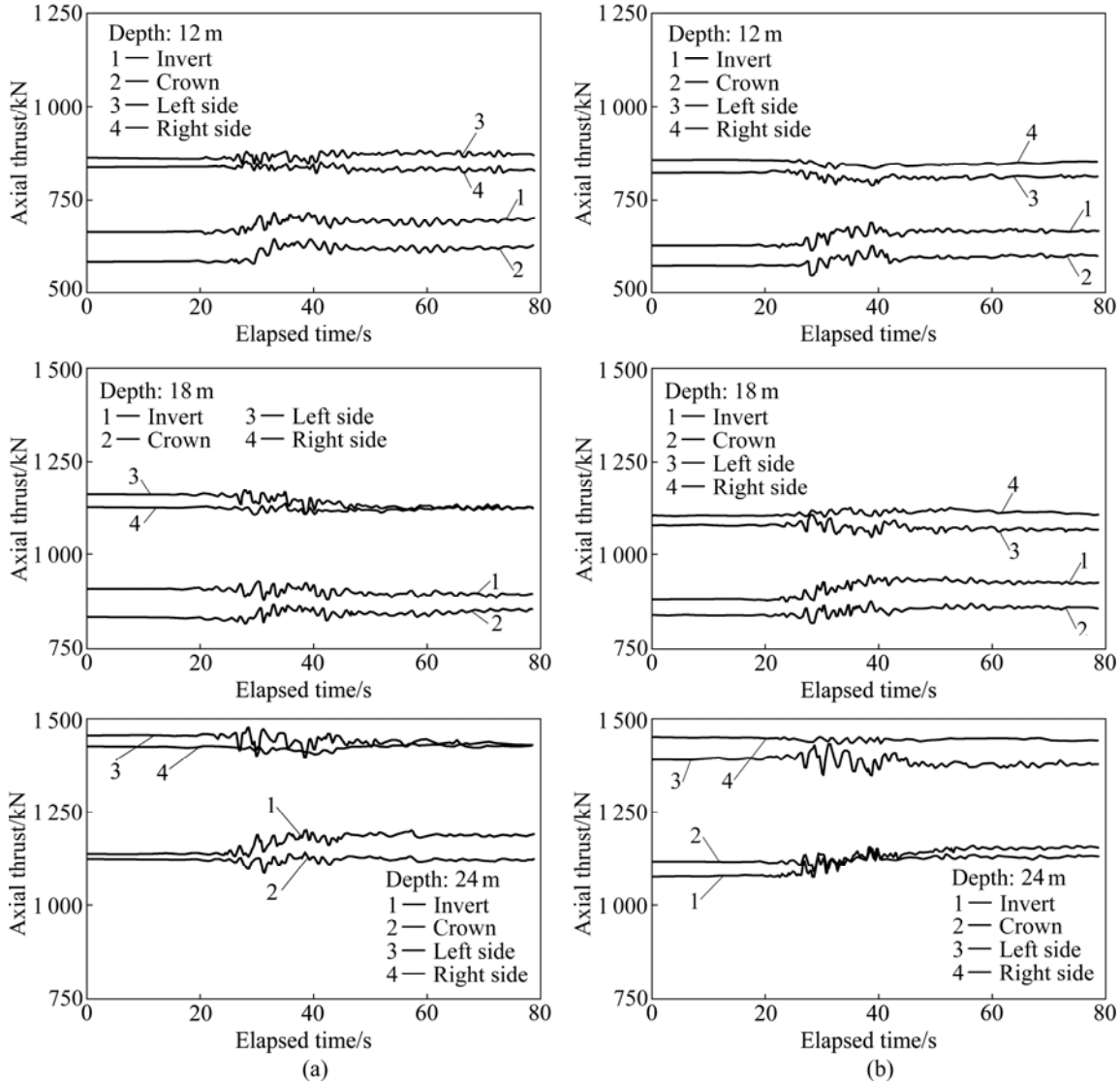

Fig.3 Time history of lining axial thrust for horizontally placed tunnels with overburden depths of 12, 18 and 24 m: (a) LHS tunnel; (b) RHS tunnel

pressure increases. For all the depths, the effect of earthquake is not clearly observed since there are only some mild fluctuations in the results.

Figure 4 shows the bending moment time history plots for the invert, crown, and left and right edges of the tunnels. In general, for each of the tunnel depth (12, 18 and 24 m), the LHS and RHS tunnels have almost the same value of initial bending moment. The initial bending moment only increases slightly as the tunnel depth increases. For each elevation, the left and right edges of the tunnel sustain the same value of bending moment; while the invert records only about half the bending moment of the crown. The variation of the bending moment between the invert and the crown increases as the tunnel depth increases. In addition, the bending moment of the tunnel invert is decreased slightly as the tunnel depth increases, but the bending moment of the tunnel crown increases as the tunnel depth increases. This may be because the lining deforms more under a higher overburden pressure and, hence, the associated bending moment increases.

The effect of earthquake is clearly observed as there are obvious fluctuations of data between 25 and 40 s in the results. The bending moment increases when the earthquake stricks but gradually decreases to either a lower value or to its original value. For the overburden of 12 m, the earthquake is actually a contributing factor because the final bending moment is found to be reduced significantly. For example, after the earthquake, the bending moments of the invert and the crown of the LHS tunnel are reduced by about 40% and 30%, respectively, while the bending moments of the left and right edges are reduced by about 35%. This reduction gets smaller as the tunnel depth increases, especially for the depth of 24 m where the final bending moments seem to remain constant throughout the elapsed time. For the 12 m-deep tunnels, this is probably due to the ease of redistribution of the soil surrounding the lining because of low confining stresses. When the overburden depth is increased to 24 m, the confining stresses of the soil are

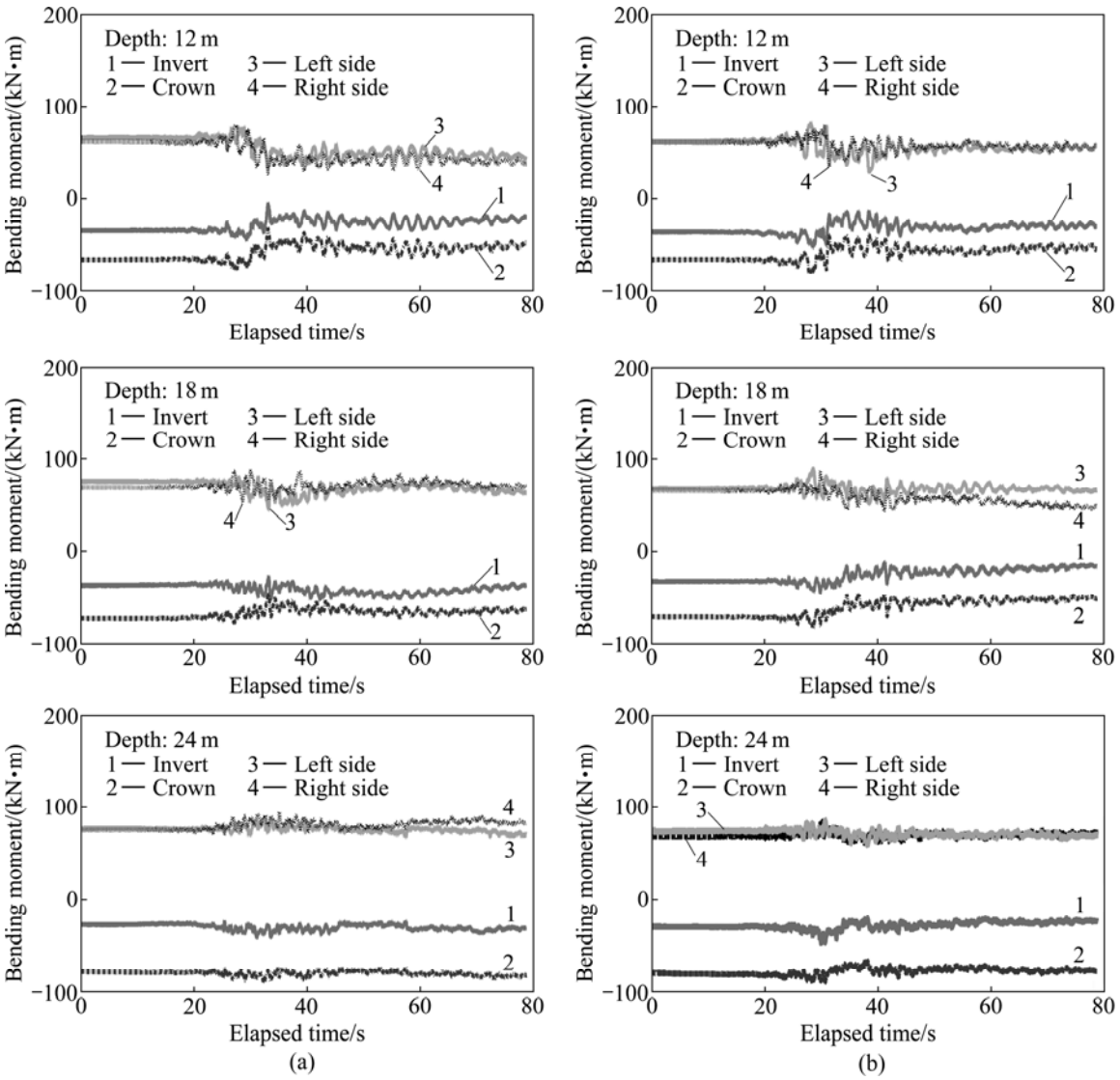

Fig.4 Time history of lining bending moment for horizontally placed tunnels with overburden depths of 12, 18 and 24 m: (a) LHS tunnel; (b) RHS tunnel

higher than those of the 12 m overburden and thus it restrains the redistribution of the soil stresses.

4.2 Effect of vertically stacked layout

Figure 5 shows the axial thrust registered at the invert, crown, and left and right edges of the tunnel. Because the upper tunnel is always located at the same depth, its axial thrust remains basically the same for all the four cases of different clear vertical spacings. As for the lower tunnel, its axial thrust corresponds to the increase of the overburden depth; and the left and right edges of the tunnel share the same value of axial thrust while the invert and the crown share another value of axial thrust. For the upper tunnel, both the left and right edges have axial thrust of about 790 kN, but the invert and the crown have axial thrusts of 708 kN and 560 kN, respectively. Hence, the self-weight of the upper tunnel contributes about 26% to the axial thrust in the invert. As

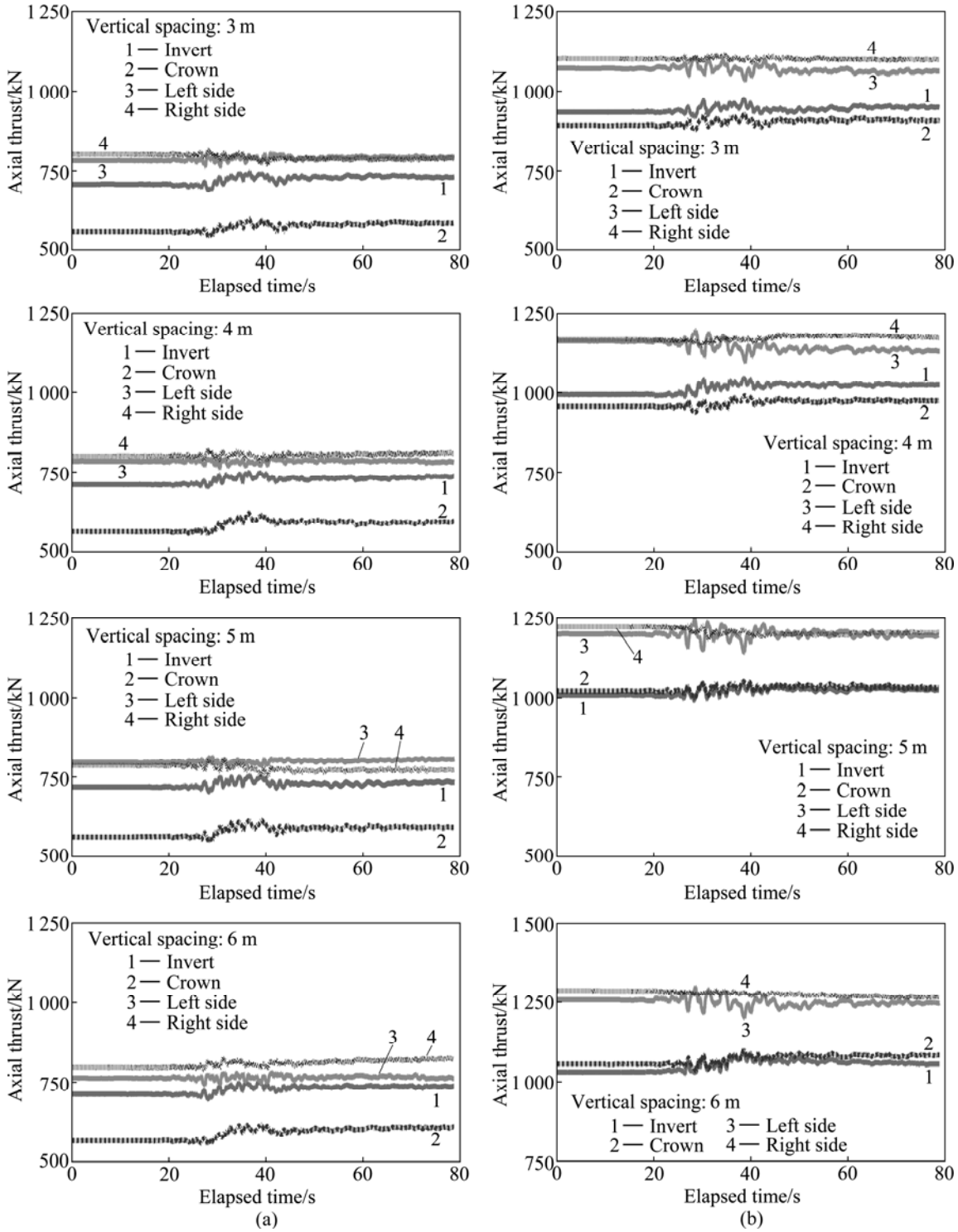

Fig.5 Time history of lining axial thrust for vertically stacked tunnels with clear vertical spacing of 3, 4, 5 and 6 m: (a) Upper tunnel; (b) Lower tunnel

for the lower tunnel, the high overburden pressure has again suppressed this contribution and, therefore, no deviation of axial thrust is observed.

Figure 6 shows the bending moment registered at the invert, crown, and left and right edges of the tunnel. For the lower tunnel, the invert and the crown have an initial bending moment of about −26 kN·m, while the left and the right edges of the lower tunnel have initial bending moment of about 22 kN·m. The initial bending moments do not vary much for the other cases of different clear vertical spacings. For the upper tunnel, the invert and the crown have initial bending moments of about −46 kN·m and −60 kN·m, respectively, while the left and the right edges have initial bending moment of about 55 kN·m. Again, the initial bending moment does not vary much for the other cases of different clear

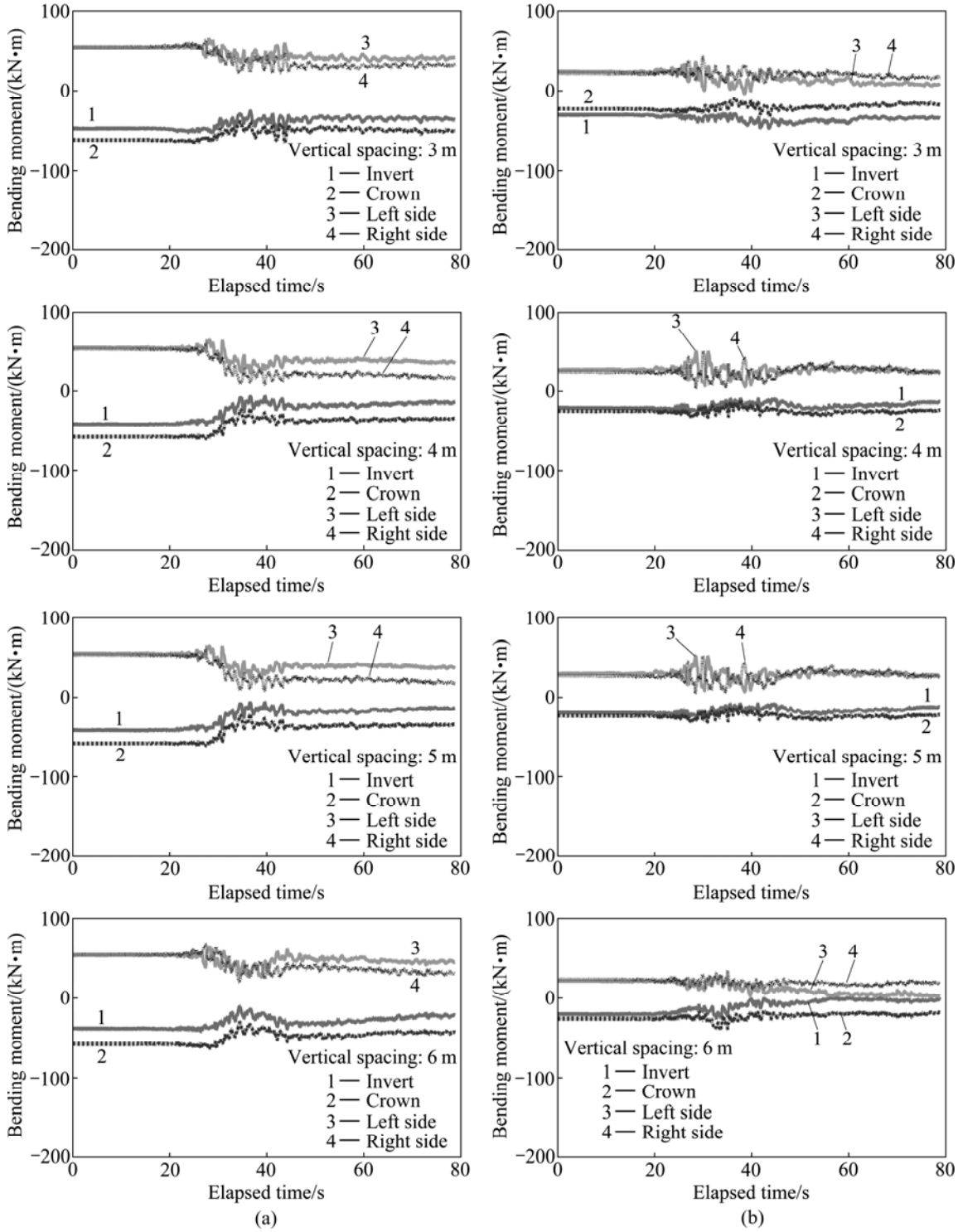

Fig.6 Time history of lining bending moment for vertically stacked tunnels with clear vertical spacing of 3, 4, 5 and 6 m: (a) Upper tunnel; (b) Lower tunnel

spacings.

During the earthquake, the effect of earthquake is not clearly seen in the axial thrust plots (Fig.5) but it is clearly felt in the bending moments plots (Fig.6) by the fluctuation of data between 25 and 40 s. The axial thrusts remain basically the same throughout the analysis, except for the very mild fluctuations of data seen during the earthquake. This is because the axial thrust is mainly contributed by the material weight above the tunnel, which is always the same at all time. The fluctuations in the bending moment plots are significantly higher than those seen in the axial thrust.

The bending moments in the lower tunnel remain about the same before and after the earthquake, but for the upper tunnel the bending moments generally decrease after the earthquake shaking. Again, this may be due to the redistribution of the soil stresses around the tunnel, which results in deformation (Fig.7) and relaxation of the upper lining that has lower confining stresses compared with the lower tunnel. Hence, the deeper the tunnel is, the less it is affected by the effect of earthquake.

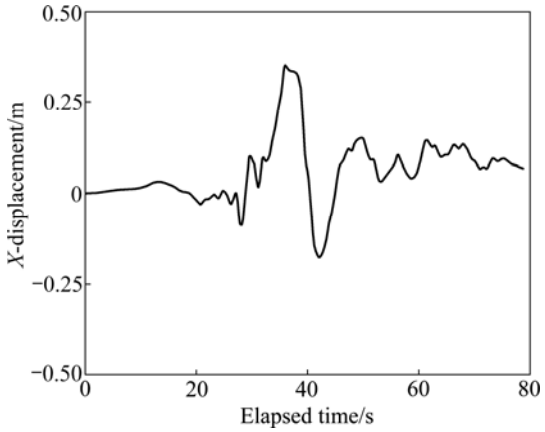

Fig.7 Time history of horizontal displacement at tunnel crown for vertically stacked tunnels with 12 m overburden

5 Conclusions

1) It can be seen that the effect of earthquake on the axial thrust of tunnel lining is not significant whether it is side-by-side or vertically stacked.

2) Immediately after the earthquake, the surrounding soils redistribute their soil pressure due to the relative deformation of the structural lining. This process results in the reduction of bending moment of the lining after the earthquake.

3) The deeper the location of the tunnel, the less the tunnel lining is affected by the effect of earthquake.

Acknowledgement

The authors are grateful to the help of Mr. Shih Hsueh-Che in the above numerical works.

References

[1] LIAO S M, LIU J H, WANG R U, LI Z M. Shield tunneling and environment protection in Shanghai soft ground [J]. Tunnelling and Underground Space Technology, 2009, 24(4): 454−465.

[2] Department of Rapid Transit Systems (DORTS), Taipei City Government. Safety considerations for the bored tunnel design and construction method [EB/OL]. http://163.29.36.51/dorts/index.jsp. 2009−07−31.

[3] Japan Society of Civil Engineering (JSCE). Japanese Standard for Shield Tunneling [S]. 3rd ed. 1996.

[4] SRAMOON A, OKAZAKI M, SUGIMOTO M. Shield tunnel lining analysis taking into account lining and ground interaction [C]// 9th National Convention on Civil Engineering. Thailand, 2004: GTE04−18.

[5] HEFNY A M, TAN F C, MACALEVEY N F. Numerical study on the behavior of jointed tunnel lining [J]. Journal of the Institution of Engineers, Singapore, 2004, 44(1): 108−118.

[6] CHEN J H, Mo H H. Mechanical behavior of segment rebar of shield tunnel in construction stage [J]. Journal of Zhejiang University: SCIENCE A, 2008, 9(7): 888−899.

[7] SHIH H C. Numerical analysis of bored tunnel lining system [D]. Taipei: Master Degree Dissertation, National Taipei University of Technology, 2004.

[8] CHOW H L, OU C Y. Boiling failure and resumption of deep excavation [J]. Journal of Performance of Construction Facilities, ASCE, 1999, 13(3): 114−120.

[9] DAS B M. Principles of soil dynamics [M]. Boston: PWS-Kent Publish-ing Co., 1993: 570.

[10] International Tunnelling Association-Working Group No.2 (ITA-WG2). Guidelines for the design of shield tunnel lining [J]. Tunnelling and Underground Space Technology, 2000, 15(3): 303−331.

[11] STEVENS D J, KRAUTHAMMER T. Analysis of blast-loaded, buried RC arch response (I): Numerical approach [J]. Journal of Structural Engineering, ASCE, 1991, 117(1): 197−212.

[12] Itasca Consulting Group, Inc. FLAC2D version 5: Fast Lagrangian Anaysis of Continua User's guide [R]. Minneapolis, USA, 2005.

[13] TAYLOR R N. Modelling of tunnel behavior [J]. Proc Institution of Civil Engineers Geotechnical Engineering, 1998, 131: 127−132.

[14] ISHIBASHI I, ZHANG X. Unified dynamic shear moduli and damping ratios of sand and clay [J]. Soils and Foundations, 1993, 33(1): 182−191.

[15] MASING G. Eignespannungen und Verfestigung beim Messing [C]// 2nd Int Congress on Applied Mechanics, Zurich, Switzerland, 1926: 332−335.

[16] PYKE R. Nonlinear soil models for irregular cyclic loading [J]. Journal of Geotechnical Engineering Division, 1979, 105(6): 715−726.

[17] VUCETIC M. Normalized behavior of offshore clay under regular cyclic loading [J]. Canadian Geotechnical Journal, 1990, 25: 33−41.

[18] HASHASH Y M A, PARK D. Non-linear one-dimensional seismic ground motion propagation in the Mississippi Embayment [J]. Engineering Geology, 2001, 62: 185−206.

[19] WOOD A M M. The circular tunnel in elastic ground [J]. Geotechnique, 1975, 25(1): 115−127.

[20] KRAMER S L. Geotechnical Earthquake Engineering [M]. NJ: Prentice Hall Inc. 1996: 653.

[21] IDRISS I M, SUN J I. User's Manual for SHAKE91: A computer program for conducting equivalent linear seismic response analyses of horizontally layered soil deposits [R]. California: University of California, Center for Geotechnical Modeling, Department of Civil and Environmental Engineering, 1992.

(Edited by YANG Bing)